The cell cycle dependent mislocalisation of emerin may contribute to the Emery-Dreifuss muscular dystrophy phenotype

Elizabeth A. L. Fairley[1,*], Andrew Riddell[2], Juliet A. Ellis[2,‡] and John Kendrick-Jones[1]

[1]MRC Laboratory of Molecular Biology, Hills Road, Cambridge, CB2 2QH, UK
[2]Wellcome Trust Centre for the Molecular Mechanism in Disease, Addenbrooke's Hospital, Cambridge, CB2 2XY, UK
*Author for correspondence (e-mail: ealf@mrc-lmb.cam.ac.uk)
‡Present address: Randall Centre for the Molecular Mechanism of Cell Function, Kings College, New Hunts House, Guy's Campus, London, SE1 1UL, UK

Accepted 24 October 2001
Journal of Cell Science 115, 341-354 (2002) © The Company of Biologists Ltd

Summary

Emerin is the nuclear membrane protein defective in X-linked Emery-Dreifuss muscular dystrophy (X-EDMD). The majority of X-EDMD patients have no detectable emerin. However, there are cases that produce mutant forms of emerin, which can be used to study its function. Our previous studies have shown that the emerin mutants S54F, P183T, P183H, Del95-99, Del236-241 (identified in X-EDMD patients) are targeted to the nuclear membrane but to a lesser extent than wild-type emerin. In this paper, we have studied how the mislocalisation of these mutant emerins may affect nuclear functions associated with the cell cycle using flow cytometry and immunofluorescence microscopy. We have established that cells expressing the emerin mutant Del236-241 (a deletion in the transmembrane domain), which was mainly localised in the cytoplasm, exhibited an aberrant cell cycle length. Thereafter, by examining the intracellular localisation of endogenously expressed lamin A/C and exogenously expressed wild-type and mutant forms of emerin after a number of cell divisions, we determined that the mutant forms of emerin redistributed endogenous lamin A/C. The extent of lamin A/C redistribution correlated with the amount of EGFP-emerin that was mislocalised. The amount of EGFP-emerin mislocalized, in turn, was associated with alterations in the nuclear envelope morphology. The nuclear morphology and redistribution of lamin A/C was most severely affected in the cells expressing the emerin mutant Del236-241.

It is believed that emerin is part of a novel nuclear protein complex consisting of the barrier-to-autointegration factor (BAF), the nuclear lamina, nuclear actin and other associated proteins. The data presented here show that lamin A/C localisation is dominantly directed by its interaction with certain emerin mutants and perhaps wild-type emerin as well. These results suggest that emerin links A-type lamins to the nuclear envelope and that the correct localisation of these nuclear proteins is important for maintaining cell cycle timing.

Key words: Emerin, Lamin A/C, Cell cycle, Protein targeting, Emery-Dreifuss muscular dystrophy

Introduction

Duchenne muscular dystrophy (DMD) and Becker muscular dystrophy (BMD) arise from genetic defects in the cytoplasmic/plasma-membrane-associated protein, dystrophin (Emery, 1996), whereas Emery-Dreifuss muscular dystrophy (EDMD) arises from genetic defects in nuclear proteins. Most cases of EDMD are inherited as an X-linked recessive trait (X-EDMD) arising from genetic defects in the inner nuclear membrane protein emerin (Bione et al., 1994), although recently the autosomal dominant (Bonne et al., 1999) and autosomal recessive (Di Barletta et al., 2000) forms of EDMD have been found to arise from genetic defects in the nuclear lamina protein, lamin A/C. These different types of muscular dystrophy are distinguished by progressive skeletal muscle wasting and cardiac abnormalities with varying severity (Emery, 1989; Emery, 1996; Funakoshi et al., 1999), but they all culminate in the breakdown of muscle-cell integrity. However, by virtue of emerin and lamin A/C being non-cytoskeletal proteins, the mechanisms that cause the loss of muscle cell integrity in EDMD must be different from those that cause DMD and BMD.

Human emerin is a serine-rich protein of 254 amino acids with a M_r of 28,993 (Bione et al., 1994). Emerin mRNA and protein studies show that emerin is ubiquitously expressed in tissues, with the highest levels in skeletal and cardiac muscle (Bione et al., 1994; Manilal et al., 1996; Nagano et al., 1996). Structural analysis predicts emerin to be a type II membrane protein, with the transmembrane region 11 residues from the C-terminus and a large hydrophilic N-terminal domain orientated towards the nucleoplasm. This N-terminal domain contains 22 potential phosphorylation sites for a large range of kinases, including those associated with cell-cycle-mediated events (Manilal et al., 1996; Nagano et al., 1996; Cartegni et al., 1997; Ellis et al., 1998). Emerin may have a role in cell-cycle-dependent events as it can occur in four different phosphorylated forms, three of which are associated with cell-cycle-dependent events (Ellis et al., 1998). Emerin possesses two regions of high sequence identity, the

transmembrane domain and LEM module (Lin et al., 2000), with two other inner nuclear membrane proteins, MAN1 and rat lamina-associated polypeptide 2 isoforms (LAP2). This observation suggests that a family of nuclear lamina-associated proteins exists that may have overlapping functions.

The inner nuclear membrane proteins bind to lamins and chromatin; for example, emerin and LAP2 have both been shown to associate with lamins (Foisner and Gerace, 1993; Furukawa and Kondo, 1998; Dechat et al., 1998; Fairley et al., 1999; Clements et al., 2000; Dechat et al., 2000a; Sakaki et al., 2001), the DNA binding protein barrier-to-autointegration factor (BAF/L2BP1) (Furukawa, 1999) and chromosomes (Shoeman and Traub, 1990; Burke, 1990; Hoger et al., 1991; Glass et al., 1993; Taniura et al., 1995; Furukawa et al., 1997; Dechat et al., 1998; Dechat et al., 2000b). Whereas LBR binds specifically to B-type lamins (Worman et al., 1990; Meier and Georgatos, 1994; Pyrpasopoulou et al., 1996; Simos et al., 1996; Maison et al., 1997; Nikolakai et al., 1997; Chu et al., 1998; Drummond et al., 1999), chromatin and the chromodomain protein HP1 (Ye and Worman, 1996; Ye et al., 1997; Duband-Goulet and Courvalin, 2000). These inner nuclear membrane proteins that form part of protein complexes at the nuclear envelope are therefore thought to have a structural role in maintaining nuclear architecture and chromosomal organisation throughout the cell cycle. Regulation of the internal interactions of these protein complexes may control nuclear architecture or link the nuclear lamina to regulatory factors involved in different aspects of gene expression.

During the cell cycle, at prometaphase, when nuclear envelope disassembly has been completed, emerin and lamin A/C are released into the cytoplasm (Gerace and Blobel, 1980; Burke and Gerace, 1986; Vigers and Lohka, 1991; Nigg, 1992; Lourim and Krohne, 1993; Chaudhery and Courvalin, 1993; Foisner and Gerace, 1993; Maison et al., 1997; Mical and Monteiro, 1998; Broers et al., 1999; Manilal et al., 1998b; Dabauvalle et al., 1999). During mitosis, lamin A/C has a diffuse and soluble appearance, whereas emerin, being an inner nuclear membrane protein, is restricted to vesicles or ER tubules (Lourim and Krohne, 1994; Collas and Courvalin, 2000). During anaphase, emerin is observed around the surface of the chromosomes (Haraguchi et al., 2000a). By telophase, emerin and lamin A/C are redistributed over the nuclear periphery, and this occurs before nuclear import activity is regained (Dabauvalle et al., 1999). During nuclear envelope reassembly, emerin colocalises with lamin A/C but not with either LAP2, lamin-B receptor (LBR) or lamin B (Worman et al., 1988; Chaudhary and Courvalin, 1993; Nikolakaki et al., 1997; Haraguchi et al., 2000a). Together, these data suggest that the nuclear membrane components dissociate into distinct populations during mitosis, possibly to perform specific cell cycle functions. Thus emerin and lamin A/C may both be involved or required to be correctly localised for nuclear reassembly.

In X-EDMD patients, mutations occur throughout the *emerin* gene. The majority of these mutations lead to no detectable emerin by immunoblotting or immunohistochemistry in any tissue (Nagano et al., 1996; Manilal et al., 1997; Manilal et al., 1998a; Mora et al., 1997; Ellis et al., 1998; Manilal et al., 1998b; Ellis et al., 1999; Yates and Wehnert, 1999). However, there are a few reported mutations that produce modified forms of emerin, which have allowed us to make EGFP-tagged emerin constructs that mimic those found in X-EDMD patients and thus enabled us to study the function of emerin. The clinical phenotype of X-EDMD patients with null mutations is thought to be the same as the phenotype in patients expressing severely modified forms of emerin, although the missense mutation P183T was shown to be associated with a milder phenotype (Yates et al., 1999). In addition Hoeltzenbein et al. discovered heterogeneity in the distribution and severity of X-EDMD when two unrelated patients, with the same mutation, showed different phenotypes (Hoeltzenbein et al., 1999). Our previous work (Fairley et al., 1999) showed that when EGFP-emerin constructs that mimic both wild-type and modified forms of emerin were exogenously expressed in undifferentiated C2C12 mouse myoblasts, all forms were targeted to the nuclear envelope, although the mutants were targeted to a lesser extent. In all cells, overexpressed emerin was also seen in the cytoplasm to varying degrees. Interestingly, the mutant emerin Del236-241 (deletion in transmembrane region) was mainly localised in the cytoplasm, with only trace amounts at the nuclear envelope, and emerin 1-220 (deletion of transmembrane and C-terminal tail) was relocated to the nucleoplasm.

In the present paper, we have investigated the role of emerin in cell-cycle mediated events. We report here the effects that emerin mutants have on the cell cycle and the cellular distribution of both the emerin mutants and endogenous lamin A/C during and after mitosis. Cells expressing the emerin mutant Del236-241 exhibited an increase in cell-cycle length when compared with cells transfected with either wild-type or the other emerin mutants (S54F, P183T, P183H, Del95-99, 1-220). Interestingly, after a number of cell divisions, the amount of endogenous lamin A/C redistribution correlated with the level of EGFP-emerin present at the nuclear envelope. Thus cells expressing the emerin mutant Del236-241 redistributed endogenous lamin A/C to the greatest extent. Additionally, the mislocalisation of the emerin mutants and redistribution of endogenous lamin A/C were associated with alterations in nuclear envelope architecture. The nuclei in cells expressing the two deletion mutants, Del236-241 and Del95-99, were particularly affected. Since the emerin mutant Del236-241 carries the mutation in the transmembrane domain, which is important for the stability of the protein (Manilal et al., 1998a), it may explain the added severity of this mutation at the molecular level. Our results suggest that the distribution of lamin A/C is dependent on emerin being targeted to the nuclear envelope and that their correct localisation at the membrane is important for nuclear assembly and function.

Materials and Methods

Cell culture

COS-7 (green monkey kidney fibroblasts) and HeLa (Helena Lange) cells were obtained from the European Collection of Cell Lines (ECACC) and were cultured in Dulbecco's Minimal Essential Medium (DMEM; Gibco BRL) supplemented with 10% fetal bovine serum (FBS; Sigma) and 2 mM glutamine (complete medium) and were grown at 37°C in 5% CO_2.

Mutant human emerin cDNA constructs

The mutant emerin cDNA constructs were prepared as described (Fairley et al., 1999). Briefly, site-directed mutagenesis was performed on the wild-type cDNA emerin clone using PCR to incorporate mutations that are known to occur in EDMD patients and introduce restriction enzyme sites (*Hind*III at the 5′ end and *Bam*H1 at the 3′ end) for subcloning. Wild-type and mutant emerin PCR fragments were cloned into the mammalian expression vector pEGFP-C2 (Clontech) so that the enhanced green fluorescent protein (EGFP) tag was at the N-terminus of the expressed emerins. Unfortunately, the repetitive DNA sequence of emerin before residue 218 made the frame-shift 218>238 stop mutation, which was identified in an X-linked EDMD patient (Klauck et al., 1995), difficult to make by PCR so EGFP-emerin 1-220 was constructed instead. The emerin cDNA clone 1-220 (FP9) in pET-29b (Ellis et al., 1998) was subcloned into pEGFP-C1. All DNA was prepared in *Escherichia coli* DH5α cells and purified on Qiagen columns according to the QIAprep Spin Miniprep kit protocol.

Transient transfections for flow cytometry and immunofluorescence microscopy

COS-7 and HeLa cells were transfected by following the SuperFect™ Transfection Protocol from Qiagen™ using a Superfect:DNA ratio of 1:6. Subconfluent cells (60-70%) were plated out in either 75 cm^2 flasks (Orange Scientific) or coverslips (22 mm^2) in six well plates, one day before being transfected. Each 75 cm^2 flask was transfected with 6 μg of DNA, whereas each well was transfected with 2 μg of DNA. The cells were transfected for 8 hours before they were synchronised by arresting the cells in G2M with the microtubule depolymerising drug nocodazole (50 ng/ml; Sigma) diluted in complete medium for 12 hours at 37°C. Synchronised cells were then collected, washed with PBS (145 mM NaCl, 7.5 mM Na_2HPO_4, 2.5 mM NaH_2PO_4, pH 7.4), replated and grown at 37°C. Flow cytometry and immunofluorescence microscopy confirmed that these cells were arrested at G2M by the nocodazole treatment. We would have preferred to use the mouse myoblast cell line C2C12 cells rather than COS-7 cells; however, for our experiments, a large number of single cells were required, which was extremely difficult to obtain with C2C12 cells because when C2C12 myoblasts reached confluency they entered G_o and spontaneously differentiated to form myotubes.

Determination of cell-cycle profiles

COS-7 cells, which were cultured in 75 cm^2 flasks, were transfected with either EGFP-emerin constructs or EGFP-vector alone, synchronised with nocodazole, and their subsequent course through the cell cycle monitored by flow cytometry. After nocodazole treatment, cells were harvested in 0.25% trypsin (EBSS)-EDTA (0.25% trypsin; Flow Lab EBSS; 5.4 mM KCl, 0.17 M NaCl, 0.03 M $NaHCO_3$, 1.16 mM $NaH_2PO_4H_2O$, 5.55 mM D-Glucose, 1% phenol red diluted 1:4 in EDTA solution; 0.14 mM NaCl, 2.7 mM KCl, 1.5 mM KH_2PO_4, 0.5 mM EDTA, 1.12 mM $Na_2HPO_42H_2O$, pH 7.2) at time points 0, 3, 6, 12, 24, 28, 32 and 35 hours after treatment. The cells were spun at 129 ***g*** for 10 minutes at 4°C, washed with PBS, before being fixed in 4% paraformaldehyde for 15-20 minutes at room temperature, washed 3×PBS and permeabilised with PBS/0.2% (v/v) Triton X-100 for five minutes at room temperature. The fixation time (15-20 minutes) had no apparent effect on cells, as initially a series of fixation times were tested to determine the optimal experimental conditions. After centrifugation at 72 ***g*** for five minutes at 4°C, cells were incubated with 0.1 mg/ml RNase (Sigma) and 40 μg/ml propidium iodide (PI) 95-98% (Sigma) diluted in PBS for 30 minutes in the dark at 37°C. Thereafter cells were spun at 72 ***g*** for 10 minutes at 4°C, resuspended in PBS and passed through the flow cytometer (Becton Dickinson, San Jose, CA, USA; 1-3×10^5 cells per sample) to determine EGFP intensity and PI area. The PI area measures the intranuclear DNA content. The data were analysed for the relative number of cells in the different phases of the cell cycle using CellQuest processing and Adobe Illustrator 7.0 software.

Cell division tracking

To study the cell-cycle length of the COS-7 cells expressing the EGFP-emerin constructs over a number of cell divisions, dye-tracking experiments were performed. Transfected COS-7 cells were synchronised, as described above, prior to being labelled with the cell trafficking dye PKH26. This is a lipophilic red fluorescent marker dye that stains cell membranes and has been characterised as a useful tool for in vitro cell tracking applications (Hugo et al., 1992). The fluorescence dye intensity decreases in an exponential fashion as the dye is dispersed between the daughter cells during cell division. Determining the median fluorescent intensity of PKH26 over time allows the cell-cycle length to be monitored. Synchronised cells were harvested by trypsin-EDTA and spun at 100 ***g*** for 10 minutes at room temperature and suspended separately in serum-free media (25 μl). For each sample, equal volumes of diluent C (Sigma Kit) and 4 μM PKH26-GL fluorescent cell linker (Sigma) were added and the tubes were inverted for five minutes at room temperature. Rapid, homogenous mixing is critical for uniform labelling. The reaction was stopped by incubating the cells with 1% (w/v) BSA for one minute prior to adding an equal volume of complete medium. After centrifugation at 100 ***g*** for 10 minutes at room temperature, the cells were washed once with complete medium, before being resuspended in complete medium. One third of each sample was then passed through the flow cytometer (Becton Dickinson; 1-2×10^5 cells per sample) to determine the PKH26 fluorescent intensity of the cells at time 0. The remaining cell samples were resuspended in complete medium and replated into tissue culture flasks. The cells were left to adhere for eight hours prior to the PKH26 intensity being remeasured after passing through both two and four cell divisions. From experiments using PI, the cell-cycle length of COS-7 cells transfected with wild-type EGFP-emerin was found to be 22±1 hours. By 24 hours, all the cells had returned to G1, therefore 24 hours was taken to be representative of one cell division. Two cell divisions was calculated as 8 hours (cell recovery time) plus 2×24 hours=56 hours and 4 cell divisions as 56 hours plus 2×24 hours=104 hours. To determine the median PKH26 intensity, the flow cytometry data were analysed by CellQuest processing and Adobe Illustrator 7.0 software. Cell viability at each time point was calculated on a duplicate cell sample using the trypan blue dye exclusion test for cell viability (Metcalf et al., 1996).

To determine the cell-cycle length of COS-7 cells transfected with wild-type and Del236-241 EGFP-emerins, the cycling rates (decrease in fluorescent dye intensity per hour) were calculated using the exponential rate constant equation; rate constant (R)=[-ln (intensity)/(initial intensity)]/time (hours).

Immunofluorescence microscopy

For microscopic visualisation of COS-7 cells during interphase, cells were plated onto coverslips, transfected with either EGFP-emerin constructs or EGFP-vector alone, as described above and then washed three times in PBS prior to being fixed in 4% (w/v) paraformaldehyde for 15-20 minutes at room temperature. To study the cellular location of nuclear proteins during and after mitosis, COS-7 and HeLa cells were plated onto coverslips, transfected, synchronised with nocodazole as described previously, washed in PBS and incubated for 0.5, 1, 3, 6, 12, 24, 28 and 35 hours at 37°C and then washed three times PBS and fixed in 4% (w/v) paraformaldehyde for 15-20 minutes at room temperature.

All fixed cells were washed three times in PBS, permeabilised in PBS/0.2% (v/v) Triton X-100 for 5 minutes, washed three times in PBS and blocked with PBS/0.2% (w/v) fish gelatin (Sigma) for 4×10

minutes prior to being incubated with either the primary monoclonal antibody, α-tubulin at 1:500 (Sigma) or anti-lamin A/C 1:10 (Jol 2; a kind gift from C. J. Hutchison) for 60 minutes in a humidified chamber. Anti-lamin A/C does not distinguish between the two alternative spliced proteins of the *lamin A* gene. The cells were washed thoroughly for 4×10 minutes with PBS/fish gelatin and incubated with the secondary antibody, sheep anti-mouse IgG 1:100 (Amersham Life Sciences), for 30 minutes in a humidified chamber. Thereafter the coverslips were washed thoroughly for 3×10 minutes in PBS/fish gelatin and three times in PBS for 5 minutes, rinsed in deionised water and mounted in DAPI mounting medium (2 μg/μl of pd-DAPI; 1 μg/μl p-phenylenediamine, 0.05 mg/ml DAPI, 90% glycerol in PBS diluted 1:1000 in Mowiol mounting medium; 87% (v/v) glycerol, 0.2M Tris-HCL pH 8.5, 12% (w/v) Mowiol; Calbiochem) on slides which were then washed in 70% methanol and air dried.

Immunofluorescence microscopy was performed on a Nikon type 108 microscope using a Nikon PlanApo 63× lens, numerical aperture of 1.4 and a triple dichroic filter (emission filters; DAPI 479, Texas Red 605, GFP 522). Images were taken sequentially at 1.0 second exposure and processed by IPlab, Adobe Photoshop 4.0 and QuarkXpress 4.0 software.

Transfected COS-7 and HeLa cells, synchronised and incubated on coverslips for 28 and 35 hours, were examined by the Radiance Confocal Laser Scanning System (BioRad) to determine the extent of colocalisation of endogenously expressed lamin A/C and exogenously expressed emerin. Scanning was done using a Nikon Plan Apo 100× lens, numerical aperture 1.4 and a double dichroic filter (dichroic mirrors; 560 DCLP and 650 DCLP) using argon 488 nm, emission filter; HQ 515/30 nm and GreNe 543 nm, emission filter; 590/70 nm. A series of 0.2 μm z-sections were taken sequentially and the data were collected by using lasersharp 2000 software (BioRad) and processed by mrc2M (Michio Ono; email micono@tky.threeweb.ne.jp), Adobe Photoshop 4.0 and QuarkXpress 4.0 software.

The quantification of COS-7 and HeLa cells, which was performed 28 hours after synchronisation, was done on the Radiance Confocal Laser Scanning System (BioRad) using a Nikon Plan Apo 40× lens with a numerical aperture of 1.3. The immunofluorescently labelled cells that were overexpressing emerin were excluded from analysis.

Results

Effect of mutant emerins on the cell cycle length of COS-7 cells

Since our previous studies had shown a significant difference in localisation between wild-type and the mutant forms of emerin (S54F, P183T, P183H, Del95-99, Del236-241, 1-220) when expressed in undifferentiated C2C12 cells (Fairley et al., 1999), we wanted to see whether the length of the cell cycle in cells expressing wild-type EGFP-emerin (1-254) was different from that in cells expressing these mutant forms of emerin. Initially, it was important to establish the length of the cell cycle in untransfected COS-7 cells so that we could check the cell cycle length of COS-7 cells transfected with EGFP-emerin constructs. Propidium Iodide (PI) was used so that the DNA content of cells could be determined using flow cytometry. The asynchronised profile of COS-7 cells is shown in Fig. 1A; the black line shows that the majority of cells were in the G1 stage of the cell cycle. After the cells were treated with nocodazole, a microtubule-depolymerising drug, the majority of cells were arrested in G2M; the blue line in Fig. 1A shows at least 50% synchronisation.

To determine the length of one cell cycle, untransfected and transfected, COS-7 cells were released from G2M by washing out the nocodazole and samples of cells collected at specific time points (0, 3, 6, 12, 24, 28, 32 and 35 hours). At each time point, the DNA content (PI area) and EGFP intensity could be measured by flow cytometry (Fig. 1B). The untransfected population (dotted black line) and transfected population (solid black line) could be gated to allow each population to be analysed separately. The gates allowed cell doublets or cells expressing a high amount of EGFP to be excluded from analysis. The flow-cytometry results were represented as cell-cycle profiles (Fig. 1C) to show the relative number of cells in the specific cell-cycle stages (G1, S or G2M) for each of the sample populations (untransfected and transfected). In each profile the orange lines represent the untransfected populations and the green and red lines represent cells expressing EGFP-emerin 12 and 24 hours after being released from G2M. These results indicate that the untransfected COS-7 cells took 22 hours (±1 hour) to complete one cell cycle. By using the untransfected population as an internal control, we showed that cells expressing wild-type or the mutant emerins, except for those expressing Del236-241, moved through the cell cycle at the same rate as the untransfected cells. The cell-cycle profiles are shown for wild-type emerin (1-254), S54F, Del236-241 and 1-220 emerin at 12 and 24 hours; the profiles for S54F accurately represents the data from the other emerin mutants P183H, P183T and Del95-99 (Fig. 1C). Cells expressing the mutant emerin construct Del236-241 had a prolonged cell-cycle length, an effect first seen 12 hours after synchronisation. At this point, the untransfected cells (G1-S) had a different cell-cycle profile from cells expressing Del236-241 (G1). The lag was more evident at 24 hours, where the cells transfected with the mutant Del236-241 were still in S-G2M, whereas the untransfected and other transfected populations were moving from G2/M to G1. These results indicate that the emerin mutant Del236-241, which has been shown to be the most severely mistargeted emerin mutant (Fairley et al., 1999), caused the cell cycle to lag. Flow cytometry experiments were also carried out using HeLa cells, which have a similar cell cycling time to COS-7 cells, to show that the effect seen in COS-7 cells transfected with Del236-241 EGFP-emerin was not cell-type specific (data not shown).

To establish the extent of the lag in the cell cycle caused by the emerin mutant Del236-241, cells were transfected with either wild-type or mutant EGFP-emerins and monitored over a number of cell divisions using a fluorescent cell tracking dye (Fig. 2). The fluorescent cell-tracking dye was incorporated into cell membranes at time zero, and its intensity examined at three time points (0, 56 and 104 hours) by flow cytometry. The cell-cycle length was determined by plotting the median fluorescent dye intensity over time. Exponential curves were observed for untransfected COS-7 cells and COS-7 cells transfected with all the EGFP-emerin constructs except Del236-241. Exponential curves were expected because the fluorescence-dye intensity decreases as the dye is dispersed between the daughter cells during cell division, and the number of cell divisions decreases as the cells reach confluency. The cells expressing EGFP-emerin mutant Del236-241 showed that the lag continued through successive rounds of the cell cycle as there was a steady linear decrease in the fluorescent dye intensity with time (Fig. 2; solid blue line). The percentage of viable cells (untransfected and transfected) in each sample was determined by using a trypan blue stain. The values obtained,

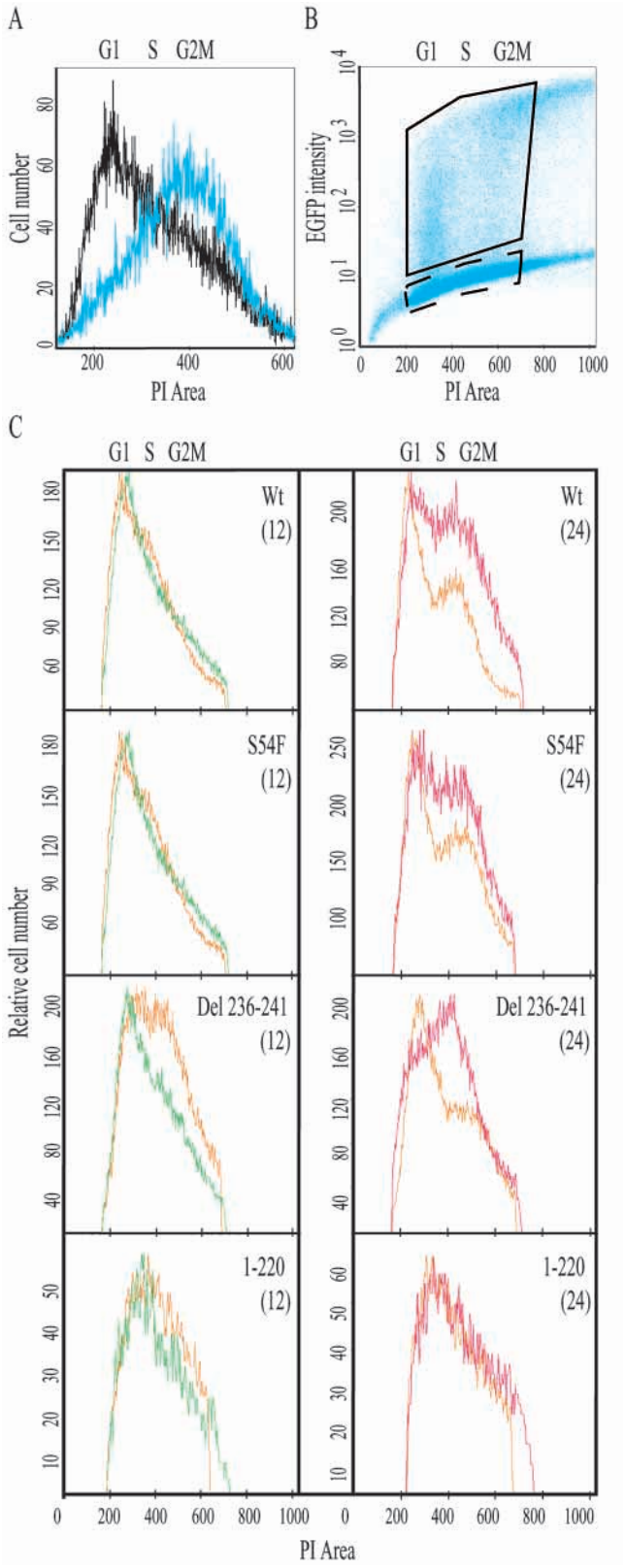

Fig. 1. (A) Cell cycle profiles of asynchronised and synchronised COS-7 cells. Propidium Iodide (PI) was added to COS-7 cells so that their DNA content could be measured by flow cytometry, and thus the stages of the cell-cycle identified. The black line shows the cell-cycle profile for asynchronised COS-7 cells. The cells are in G1, S and G2M phase, although the majority of the cells are in G1. Cells were synchronised by nocodazole treatment; the blue line shows that now at least 50% of cells are arrested in G2M. (B) Flow cytometry can be used to study EGFP-tagged proteins during the cell cycle. COS-7 cells were transfected with EGFP-emerin constructs and examined by flow cytometry. The untransfected population (dotted black line box) and transfected population (solid black line box) could be gated to allow each population to be analysed separately. The gates also allowed doublet cells or cells expressing a high amount of EGFP to be excluded from the analysis. (C) Cell-cycle profiles of untransfected and EGFP-emerin-transfected cell populations. The PI area (DNA content) and EGFP intensity were both monitored so that cell-cycle profiles show the relative number of cells in G1, S or G2M for each population (untransfected and transfected). In each profile, the orange lines represent the untransfected populations and the green and red lines represent cells expressing EGFP-emerin 12 and 24 hours after being released from G2M. The untransfected population acts as an internal control to compare the length of the cell cycle with that for cells transfected with either wild-type or mutant forms of emerin. The cells expressing the emerin mutant Del236-241 are shown to have a prolonged cell cycle length.

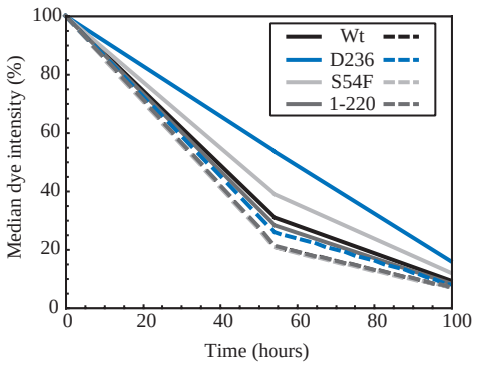

Fig. 2. Tracking untransfected and transfected cells over a number of cell divisions. To establish the extent of the lag caused by EGFP-emerin mutant (Del236-241), COS-7 cells transfected with EGFP-emerin constructs were monitored over four cell divisions using a fluorescent cell-tracking dye (PKH26). The fluorescent cell-tracking dye was incorporated into cell membranes at time 0, and its intensity examined at three time points 0, 56 and 104 hours. For the untransfected populations (wt, black dotted line; D236 (D236-241), blue dotted line; S54F, light-grey dotted line; 1-220, dark-grey dotted line), the fluorescence dye intensity decreases exponentially as the dye is dispersed between the daughter cells during cell division. Thus, the medium fluorescent intensity of PKH26 over time allows the cell-cycle timing to be monitored. Cells transfected with wild-type EGFP-emerin (black solid line) or mutants; missense S54F (light-grey solid line) and 1-220 (dark-grey solid line) showed the normal exponential decrease in dye intensity, whereas cells transfected with EGFP-emerin mutant Del236-241 (D236, blue solid line) show a steady decrease in dye intensity, meaning that these cells took longer to cycle.

90.65-98.30%, indicated that the cells were unaffected by the EGFP expression and tracking dye treatment.

To compare the cell-cycle length of COS-7 cells transfected with wild-type and Del236-241 EGFP-emerins, the cycling rates (decrease in fluorescent dye intensity per hour) were calculated. The cycling rate for cells transfected with wild-type EGFP-emerin was 25.60 arbitrary units of

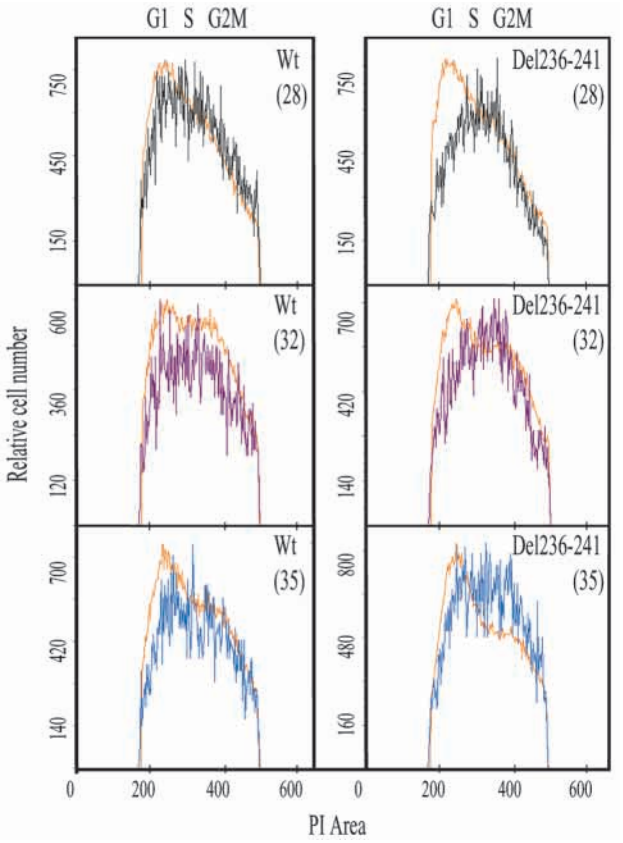

Fig. 3. Cell-cycle profiles showing cells expressing wild-type and Del236-241 EGFP-emerin at the same stage in the cell cycle. The PI area (DNA content) and EGFP intensity were both monitored so that cell-cycle profiles show the relative number of cells in G1, S or G2M for each population (untransfected and transfected). In each profile, the orange lines represent the untransfected populations and the black, purple and blue lines represent cells expressing EGFP-emerin 28, 32 and 35 hours after being released from G2M. Cells expressing wild-type EGFP-emerin 28 hours after synchronisation were in G1-S, whereas cells expressing Del236-241 EGFP-emerin 35 hours after synchronisation were in G1-S. Thus cells expressing Del236-241 EGFP-emerin lag behind those cells expressing wild-type EGFP-emerin by six to seven hours per cycle.

fluorescent dye intensity per hour, whereas for cells transfected with Del236-241, EGFP-emerin was 20.24 arbitrary units of fluorescent dye intensity per hour. As we have shown (Fig. 1) that COS-7 cells untransfected or transfected with wild-type or all the mutant emerins (S54F, P183T, P183H, Del95-99, 1-220), except for emerin mutant Del236-241, complete two cell division by 24 hours, we can calculate using the cycling rates that cells transfected with Del236-241 EGFP-emerin cycle six to seven hours slower. Thus, we could determine when cells expressing wild-type EGFP-emerin were at the same stage in the cell cycle as cells expressing Del236-241 EGFP-emerin. Cell-cycle profiles (Fig. 3) show that cells transfected with either wild-type or the mutants (S54F, P183T, P183H, Del95-99, 1-220) were in G1-S, whereas cells transfected with Del236-241 EGFP-emerin were still in S-G2M 28 and 32 hours after synchronisation. However, 35 hours after synchronisation, cells transfected with Del236-241 EGFP-emerin were in G1-S, demonstrating that cells expressing this mutant lag six to seven hours behind, per cell cycle, when compared with cells expressing wild-type EGFP-emerin.

Fig. 4. The localisation of emerin mutants through mitosis by immunofluorescence microscopy. To show simultaneously the location of exogenously expressed mutant forms of emerin and endogenous lamin A/C during mitosis, COS-7 cells were transfected with wild-type (A), missense S54F (B), Del236-241 (C) and 1-220 (D) EGFP-emerins and immunolabelled for lamin A/C. The chromatin was stained with DAPI to identify the stages in the cell cycle. The cells expressing wild-type and mutant EGFP-emerins, except for Del236-241, show a similar mitotic distribution to that of endogenous lamin A/C. The cells expressing the emerin mutant Del236-241 show an altered localisation pattern for both the EGFP-emerin and endogenously expressed lamin A/C. Cells transfected with EGFP-emerin 1-220 were similar to those transfected with EGFP-vector alone. Nikon type 108 microscope; bar, 10 μm.

Intracellular distribution of emerin mutants and endogenous lamin A/C during and after mitosis

In parallel with the flow cytometry experiments, we monitored the cellular distribution of wild-type and mutant forms of emerin and endogenous lamin A/C during and after mitosis by immunofluorescent microscopy. Initially, using synchronised cells expressing wild-type EGFP-emerin labelled with an α-tubulin antibody and DAPI, we observed that our expressed wild-type EGFP-emerin followed the distribution of endogenously expressed emerin during mitosis as previously demonstrated (Manilal et al., 1998b; Dabauvalle et al., 1999; Haraguchi et al., 2000a). We then examined the distribution of endogenously expressed lamin A/C and the exogenously expressed wild-type and mutant forms of EGFP-emerin (S54F, P183T, P183H, Del95-99, Del236-241, 1-220) through mitosis (Fig. 4). We observed that endogenous lamin A/C, wild-type and all mutant forms of EGFP-emerin, except for 1-220 and Del236-241 EGFP-emerin, were dispersed into the cytoplasm during prometaphase; during anaphase they localised around the decondensing chromatin and concentrated at the cleavage furrow; whereas at telophase they relocalised to the nuclear membrane. The cells expressing the emerin mutant S54F (Fig. 4B) represent the results that were obtained with the other emerin mutants P183T, P183H or Del95-99. Thus, our transfectants expressing wild-type and mutant EGFP-emerins S54F, P183T, P183H, Del95-99 showed a similar mitotic distribution to that of endogenous lamin A/C. When cells were transfected with 1-220 EGFP-emerin (Fig. 4D), the distribution patterns were similar to those seen when cells were transfected with EGFP-vector alone. Cells transfected with Del236-241 EGFP-emerin at interphase (Fig. 4C) showed this mutant to be mainly localised in the cytoplasm with only trace amounts at the nuclear envelope when compared to wild-type (Fig. 4A). At prometaphase, EGFP-emerin Del236-241 and lamin A/C showed a diffuse cytoplasmic distribution pattern. However, at metaphase this emerin mutant concentrated at specific points around the chromosomes on the metaphase plate, and at anaphase less of it was seen around the chromosomes or at the cleavage furrow during telophase. Interestingly, at cytokinesis this emerin mutant was shown to redistribute endogenously expressed

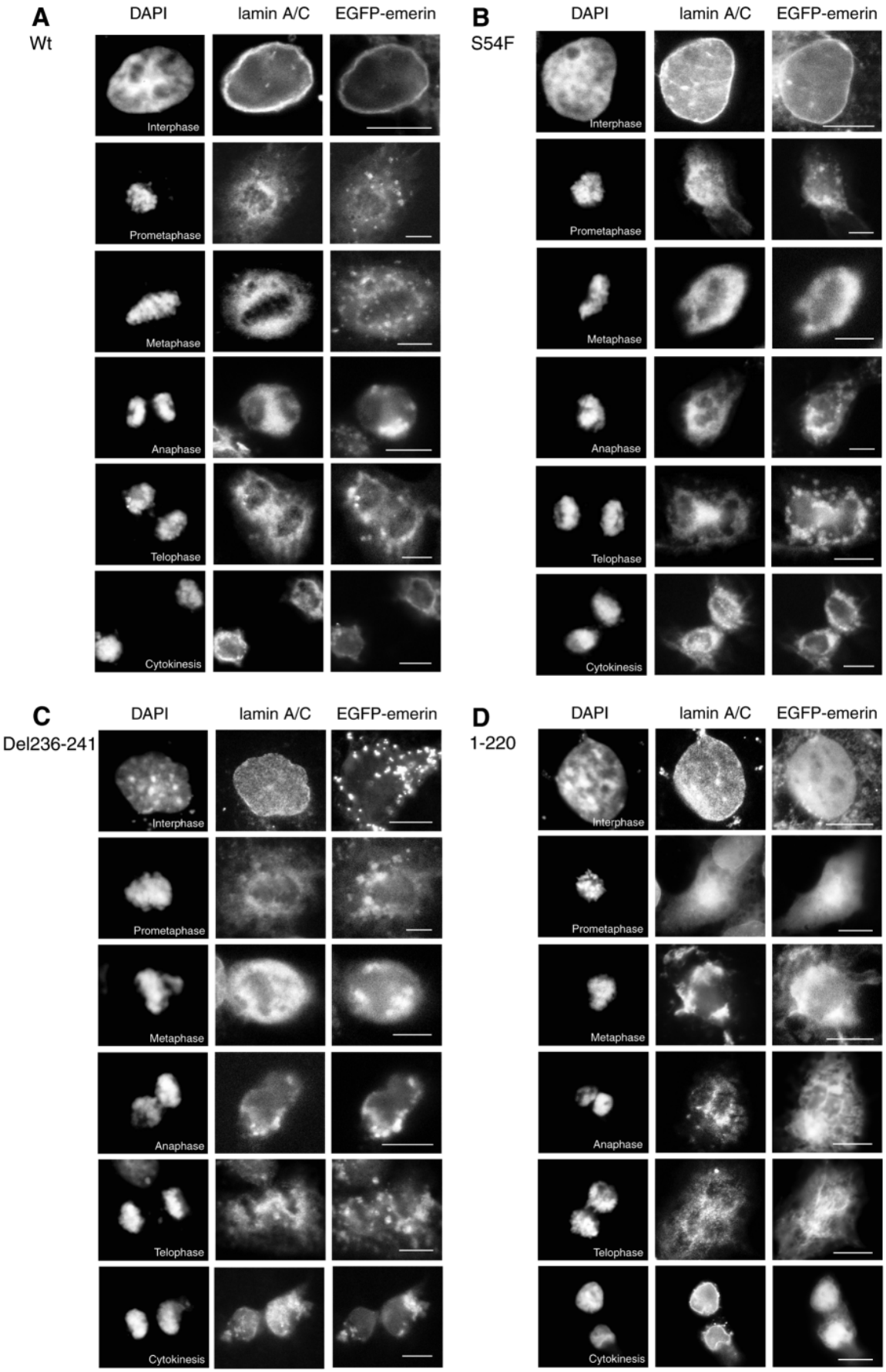
A
Wt
DAPI
lamin A/C
EGFP-emerin
Interphase
Prometaphase
Metaphase
Anaphase
Telophase
Cytokinesis
B
S54F
DAPI
lamin A/C
EGFP-emerin
Interphase
Prometaphase
Metaphase
Anaphase
Telophase
Cytokinesis
C
Del236-241
DAPI
lamin A/C
EGFP-emerin
Interphase
Prometaphase
Metaphase
Anaphase
Telophase
Cytokinesis
D
1-220
DAPI
lamin A/C
EGFP-emerin
Interphase
Prometaphase
Metaphase
Anaphase
Telophase
Cytokinesis

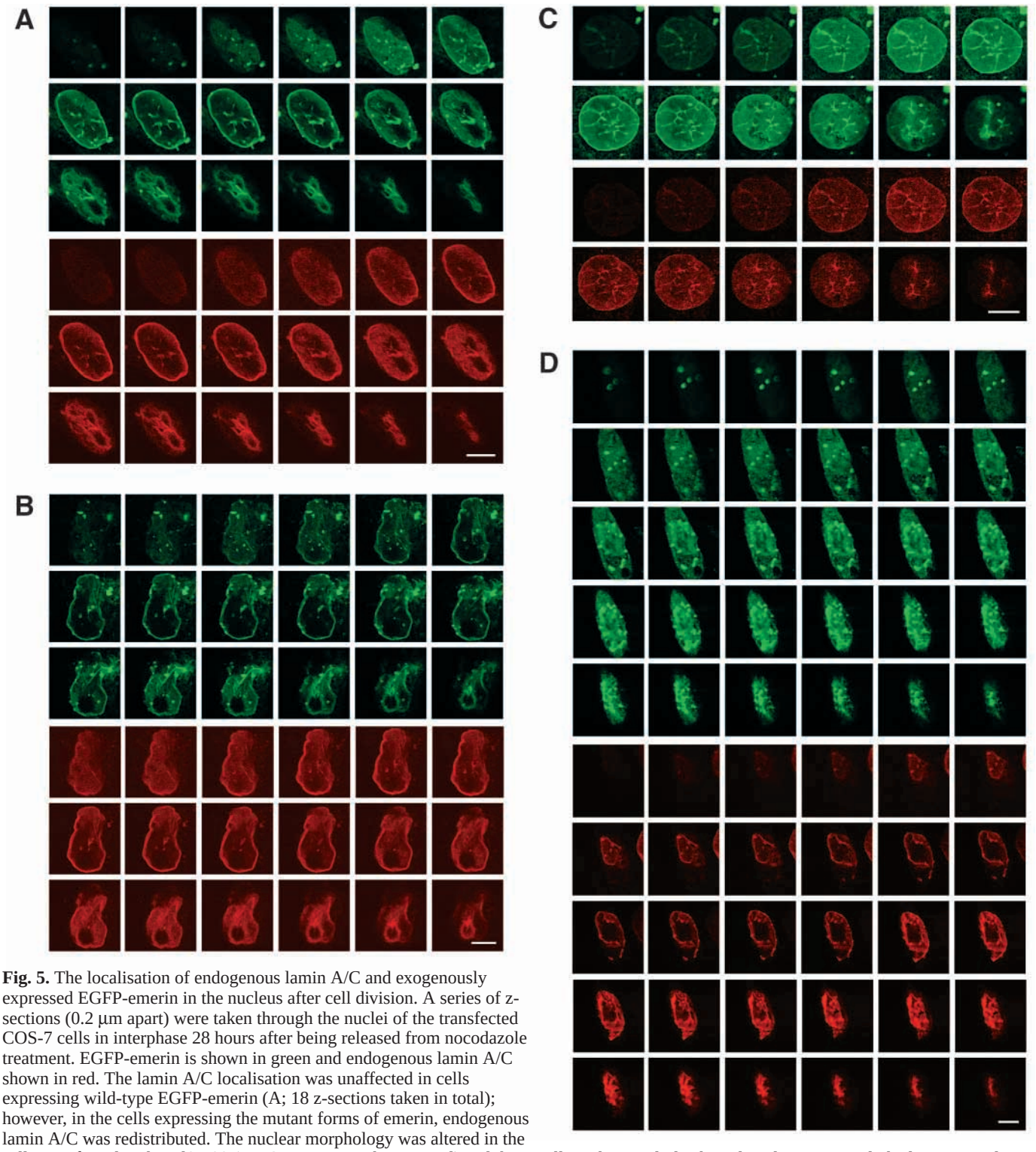

Fig. 5. The localisation of endogenous lamin A/C and exogenously expressed EGFP-emerin in the nucleus after cell division. A series of z-sections (0.2 μm apart) were taken through the nuclei of the transfected COS-7 cells in interphase 28 hours after being released from nocodazole treatment. EGFP-emerin is shown in green and endogenous lamin A/C shown in red. The lamin A/C localisation was unaffected in cells expressing wild-type EGFP-emerin (A; 18 z-sections taken in total); however, in the cells expressing the mutant forms of emerin, endogenous lamin A/C was redistributed. The nuclear morphology was altered in the cells transfected with Del95-99 (B; 23 z-sections taken in total) and those cells with irregularly shaped nuclei consistently had exogenously expressed Del95-99 EGFP-emerin and endogenously expressed lamin A/C lost from one of the poles. The nuclear morphology was also altered in cells that expressed Del236-241 (D; 31 z-sections taken in total) EGFP-emerin, and the number of z-sections show that the cells expressing this mutant were smaller and rounder. Intranuclear tubules of emerin and lamin A/C are seen to a greater extent in cells transfected with either wild-type (A) or missense mutations (C; S54F). Radiance Confocal Laser Scanning System; bar, 5 μm.

lamin A/C into the cytoplasm. Thus, after one cell division, the mutant form of emerin Del236-241 causes a redistribution of endogenous lamin A/C in a cell-cycle-dependent manner.

To investigate the redistribution of lamin A/C, we examined cells 28 and 35 hours after synchronisation. From our flow cytometry results (Fig. 3), we established that cells expressing

wild-type EGFP-emerin 28 hours after synchronisation were at the same stage in the cell cycle as cells expressing Del236-241 EGFP-emerin 35 hours after synchronisation. To determine the extent of colocalisation of endogenous lamin A/C and exogenously expressed emerin, a series of z-sections were taken (0.2 μm apart) through transfected cells using the Radiance Confocal Scanning System (Fig. 5). We observed that the lamin A/C localisation was unaffected in cells expressing wild-type EGFP-emerin (Fig. 5A), whereas in the cells expressing all the mutant emerin forms, endogenous lamin A/C was redistributed to different extents. The most severe endogenous lamin A/C redistribution was seen in cells expressing emerin mutant construct Del236-241 (Fig. 5D) followed by cells expressing the mutant Del95-99 (Fig. 5B). In cells expressing emerin constructs S54F, P183H and P183T, lamin A/C distribution was least affected, as shown in Fig. 5C. The nuclear envelope architecture was also altered in the cells transfected with EGFP-emerin Del95-99 and Del236-241 (Fig. 5B, D). Interestingly, cells expressing Del95-99 EGFP-emerin (Fig. 5B) with irregularly shaped nuclei consistently had exogenously expressed emerin and endogenously expressed lamin A/C lost from one of the poles, and the cells expressing Del236-241 EGFP-emerin (Fig. 5D) appeared to be fewer, smaller and rounder (cell shrinkage) with cytoplasm condensation. Intranuclear foci/tubules of exogenously expressed emerin and endogenous lamin A/C were seen to a greater extent in cells transfected with wild-type or missense mutations (Fig. 5A, C) when compared to cells transfected with the emerin mutants Del236-241, Del95-99 or 1-220. These z-sections show that the targeting of wild-type and mutant emerin were in agreement with our previous localisation studies (Fairley et al., 1999). Thus, all the mutant forms of emerin were mistargeted to varying degrees, and as a consequence the endogenous lamin A/C was similarly mislocalised after the completion of cell division.

In COS-7 and HeLa cells transfected with wild-type, Del236-241 and S54F EGFP-emerins, the percentage of cells in which endogenous lamin A/C was redistributed and the nuclear morphology was affected 28 hours after synchronisation was determined (Fig. 6; Table 1). The endogenous lamin A/C and nuclear architecture appeared unaffected in either COS-7 or HeLa cells transfected with wild-type EGFP-emerin. The number of cells transfected with either Del236-241 or Del95-99 EGFP-emerin that had irregularly shaped nuclei with lamin A/C mislocalised were greater than those cells that had round-shaped nuclei with lamin A/C localised. No quantification data were obtained for cells expressing either P183T or P183H EGFP-emerin, although from measuring the cells expressing S54F EGFP-emerin we can predict that cells expressing these missense mutations would be similar. The quantification data conclude that, after cell division, the correct localisation of lamin A/C depends upon EGFP-emerin being targeted to the nuclear envelope.

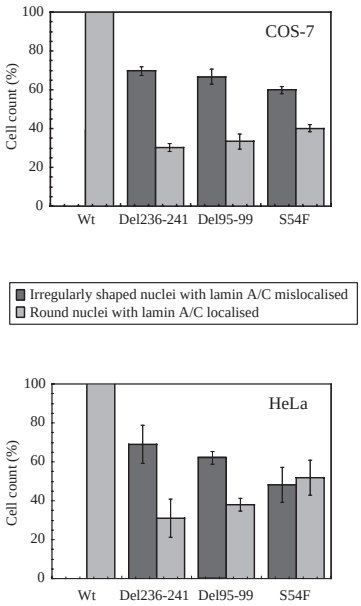

Fig. 6. A number of COS-7 and HeLa cells transfected with either wild-type or mutant EGFP-emerins show endogenous lamin A/C redistribution and altered nuclear morphology. The endogenous lamin A/C and nuclear architecture appeared unaffected (100%) in both COS-7 or HeLa cells transfected with wild-type (wt) EGFP-emerin (COS-7; *n*=3, an average of 857 cells per count, HeLa; *n*=3, an average of 691 cells per count). The number of cells transfected with either Del236-241 (COS-7; *n*=3, an average of 595 cells per count, HeLa; *n*=3, an average of 124 cells per count) or Del95-99 (COS-7; *n*=3, an average of 1169 cells per count, HeLa; *n*=3, an average of 852 cells per count) EGFP-emerin that had irregularly shaped nuclei with lamin A/C mislocalised was greater than the number of cells that had round nuclei with lamin A/C localised. The percentage of cells expressing S54F EGFP-emerin (COS-7; *n*=3, an average of 1204 cells per count; HeLa; *n*=3, an average of 713 cells per count) that had either irregularly shaped nuclei with lamin A/C mislocalised or round-shaped nuclei with lamin A/C localised was similar. The quantification data show that, after cell division, the redistribution of lamin A/C depends upon the localisation of EGFP-emerin.

Intranuclear foci/tubules and cytoplasmic localisation of emerin and lamin A/C

To examine the localisation of expressed emerin and

Table 1. The comparison between the percentages of cells transfected with either wild-type or mutant EGFP-emerin which show either irregular-shaped nuclei with lamin A/C localised or round-shaped nuclei with lamin A/C localised

	Del236-241 % (s.e.m.)	Del95-99 % (s.e.m.)	S54F % (s.e.m.)
Nuclear morphology of COS-7 cells			
Irregular-shaped nuclei with lamin A/C mislocalised	69.75 (2.21)	66.66 (3.77)	59.89 (1.78)
Round-shaped nuclei with lamin A/C localised	30.25 (2.21)	33.34 (3.77)	40.11 (1.78)
Nuclear morphology of HeLa cells			
Irregular-shaped nuclei with lamin A/C mislocalised	68.98 (9.78)	62.12 (3.25)	48.16 (8.90)
Round-shaped nuclei with lamin A/C localised	31.02 (9.78)	37.88 (3.25)	51.84 (8.90)

endogenous lamin A/C in greater detail, the z-sections obtained from the Radiance Laser Scanning microscope (Fig. 5) were analysed further. Data from the centre of the nuclei, 0 and 0±5 μm, in the x-y direction, were obtained from all the z-sections taken for a specific cell. They were collected and represented as a x-z slice through the cell (Fig. 7). Wild-type EGFP-emerin was localised at the nuclear envelope and as intranuclear foci/tubules; both of which colocalised with endogenous lamin A/C (Fig. 7A). Interestingly, the x-z slices of cells expressing the Del236-241 EGFP-emerin showed that this mutant form of emerin was localised in the cytoplasm and at concentrated areas around the nuclear envelope 28 (Fig. 7B) and 35 (Fig. 7C) hours after synchronisation. The endogenous lamin A/C colocalised with this expressed emerin mutant in the concentrated areas around the nuclear envelope. Thus, cells expressing Del236-241 EGFP-emerin exhibited an aberrant nuclear morphology confirming the results shown in Figures 5 and 6. In combination, these results indicate the importance of emerin being correctly localised at the nuclear envelope; when emerin is mislocalised (as with the mutant forms above), the localisation of endogenous lamin A/C is altered and this leads to defects in the nuclear architecture.

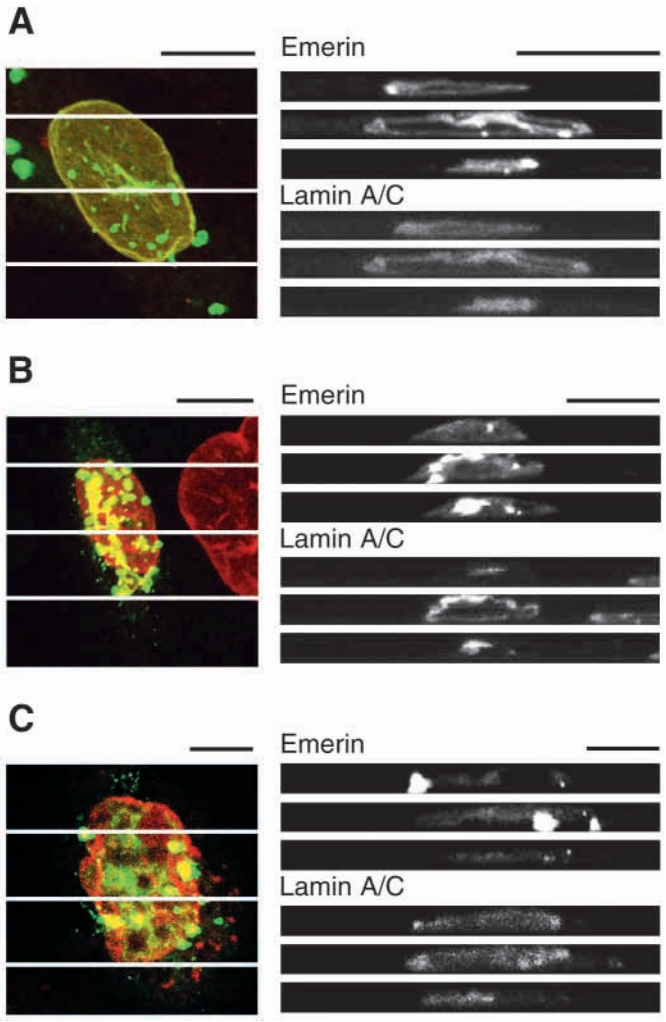

Fig. 7. Further localisation of emerin and lamin A/C by representing z-sections as x-z slices through cells. A series of z-sections (0.2 μm apart) were taken through the nuclei of COS-7 cells transfected with either wild-type or Del236-241 EGFP-emerin. The z-sections shown are for: (A) a cell transfected with wild-type EGFP-emerin (18 z-sections taken in total) 28 hours after being released from nocodazole; (B) a cell transfected with Del236-241 EGFP-emerin (31 z-sections taken in total) 28 hours after being released from nocodazole; and (C) a cell transfected with Del236-241 EGFP-emerin (25 z-sections taken in total) 35 hours after being released from nocodazole treatment. All z-sections were collected and represented as x-z slices through the cells. The projections of all the z-sections taken show emerin in green, lamin A/C in red and colocalisation in yellow. The white lines show where the z-sections were collected: the centre of the nucleus 0, 0+5 μm and 0-5 μm. The line thickness was ±0.3 μm for wild-type cells at 28 hours, ±0.3 μm for Del236-241 at 28 hours and ±0.6 μm for Del236-241 at 35 hours. Each x-z slice is shown separately in black and white for clarity. Cells expressing Del236-241 EGFP-emerin 28 and 35 hours after synchronisation were microscopically similar. The correct localisation of emerin and lamin A/C to the nuclear membrane is shown to be important, as the mutant form of emerin (Del236-241) redistributes lamin A/C with resultant defects in the nuclear architecture. Radiance Confocal Laser Scanning System; bar, 5 μm.

Discussion

In our previous studies (Fairley et al., 1999), we showed that when EGFP-emerin mutant constructs, which reflect mutations found in a number of EDMD patients, are expressed in undifferentiated C2C12 myoblasts, they were all targeted to the inner nuclear membrane but in a less efficient manner than the wild-type. The most severely mistargeted emerin mutant was Del236-241, which has a deletion in the transmembrane region. In this paper, we have shown that COS-7 cells transfected with emerin mutant Del236-241 had an increased cell-cycle length, which was six to seven hours longer per cycle, when compared to COS-7 cells untransfected or transfected with wild-type or the other mutant emerins (S54F, P183T, P183H, Del95-99, 1-220). Deletions in the transmembrane region of emerin have also been reported to decrease the stability of emerin at the nuclear envelope (Manilal et al., 1998a). Additional studies on C-terminal mutants of emerin have also suggested that a function of emerin is to provide stability to the nuclear structure (Tsuchiya et al., 1999). Thus the severe molecular defect associated with the emerin mutant Del236-241 compared with the other mutations used in these studies may explain why only this mutant produced a detectable abnormality in cell-cycle length. The mutations we studied may all cause a cell-cycle defect, but only the most severe mutation (Del236-241) was detected by the experimental system we used. Alternatively, this mutation may specifically cause a delay in the cell cycle, suggesting that particular mutations may affect the function of emerin differently.

To determine the molecular processes underlying the increase in the timing of the cell cycle associated with the emerin mutant Del236-241, the localisation of all the expressed EGFP-emerins and endogenous lamin A/C were monitored in transfected cells during and after mitosis. We demonstrated (Fig. 4) that both endogenous lamin A/C and exogenously expressed emerins (whether present at the nuclear envelope or in cytoplasmic aggregates) dispersed into the cytoplasm during nuclear envelope disassembly. Upon nuclear envelope reassembly, the expressed emerins were relocated to the nuclear envelope to the same extent as before disassembly.

However, it was observed that some lamin A/C was associated with the emerin mutant Del236-241 in the cytoplasm, suggesting that this mutant form of emerin was able to prevent lamin A/C from being correctly localised to the nuclear envelope. It should be noted that in our immunofluorescence microscopy studies, we were unable to distinguish between lamin A and C because of the specificity of the antibody used (see Materials and Methods). Furthermore, detailed examination of cells that had under gone division showed that endogenous lamin A/C was mislocalised in cells expressing all the different emerin mutants (Fig. 5). The mislocalisation of endogenous lamin A/C correlated with the amount of emerin at the nuclear membrane. For example, the mutant emerin Del236-241, which was almost completely absent from the nuclear membrane, redistributed lamin A/C to the greatest extent. These results support previous observations that emerin and lamin A/C interact with each other in vitro (Fairley et al., 1999; Clements et al., 2000; Sakaki et al., 2001), suggesting that emerin links A-type lamins to the nuclear envelope (Hutchison et al., 2001). We therefore suggest that once the nuclear envelope has been disassembled, the expressed EGFP-emerin is able to compete with endogenous emerin for binding with endogenous lamin A and/or lamin C. It would thus appear that the emerin mutants can act in a dominant-negative manner. This is of particular interest as female carriers of X-EDMD have been described (Funakoshi et al., 1999) who exhibit dominant-negative phenotypes such as varying degrees of conduction abnormalities without muscle weakness or vice versa. The longer cell-cycle length associated with the transfectants expressing emerin mutant Del236-241 may be because the lamin A and/or lamin C in those cells is sequestered away from the nuclear envelope in sufficient quantities to impede the full function of the nuclear envelope.

To date, two models exist to explain the role of lamins during mitosis. In model one (Burke and Gerace, 1986; Dabauvalle et al., 1991; Ulitzur et al., 1992; Ellis et al., 1997; Spann et al., 1997; Ulitzur et al., 1997; Moir et al., 2000a; Moir et al., 2000b; Spann et al., 2000), lamins have been shown to interact with the nuclear-envelope components during the early stages of the reassembly process and are believed to be critical for nuclear-envelope formation. In the second model (Newport and Spann, 1987; Newport et al., 1990; Meier et al., 1991; Chaudhary and Courvalin, 1993; Jenkins et al., 1993; Wiese et al., 1997), lamins have been shown to be located in the nucleus after the nuclear envelope has been formed. However, studies (Moir et al., 2000c; Steen and Collas, 2001) revealed that A- and B-type lamins follow different pathways during nuclear assembly, suggesting that the different forms of lamin play specific roles during the cell cycle. Studies using HeLa cells indicated that the order in which proteins reassemble was emerin, LBR and several nuclear pore complex components prior to the recovery of nuclear import activity (Haraguchi et al., 2000a). Recent immunofluorescence studies (Haraguchi et al., 2000b) have suggested that BAF mediates or contributes to the localisaton of emerin during the initial stages of nuclear reassembly. Together, these results suggest that during mitosis, B-type lamins may assemble with the LBR, whereas emerin possibly assembles with A-type lamins and BAF prior to nuclear pore complex formation. Thus, the lamina plays a fundamental role in regulating nuclear assembly and chromatin organisation. However, it may be the binding partners of lamins that are critically important for the correct formation of nuclear lamina after cell division. This could explain why we do not see changes in the nuclear morphology of cells transfected with emerin mutants Del236-241 and Del95-99 (Fig. 5; Fig. 6) until after cell division. A change in nuclear morphology and a reduction in the layer of heterochromatin that lies just under the surface of the nuclear envelope has also been reported in embryonic fibroblasts taken from lamin A knockout mice (Sullivan et al., 1999), which developed a muscular dystrophy phenotype, and in muscle nuclei from X-EDMD patients that lack emerin (Fidzianska et al., 1998; Ognibene et al., 1999). The embryonic fibroblasts with no lamin A/C (*Lmna*$^{-/-}$) were irregular-shaped, elongated and exhibited a loss of B-type lamins, LAP2 and the nuclear pore complex protein Nup153 from one pole. Lamin A/C has also been shown (Collard et at., 1992) to be redistributed from one pole of the nucleus to the periphery upon differentiation. This is of interest, as nuclei of cells expressing the emerin mutant Del95-99 showed lamin A/C to be lost from one of the poles (Fig. 5). Further immunofluorescence staining of wild-type, heterozygous and null embryonic fibroblasts revealed that the loss of A-type lamins correlated with emerin mislocalisation (Sullivan et al., 1999) and in the *Lmna*-null mice: emerin was diffusely localised in the nucleus and cytoplasm, suggesting that emerin was mislocalised to the ER. Therefore, these results suggest that certain mutants may have different cell-cycle effects as the phenotypes exhibited by cells expressing the emerin mutants Del236-241 or Del95-99 were different, that is, lamin A/C being redistributed to the cytoplasm or being lost from one pole of the nucleus, respectively. Thus the absence or reduced levels of either emerin and/or lamin A/C at the nuclear envelope may cause a severe alteration in both nuclear morphology and function.

During skeletal muscle differentiation, an increase in A-type lamin expression is accompanied by changes in chromatin structure and the induction of muscle-specific gene expression (Lourim and Lin, 1989; Collard et al., 1992; Lourim and Lin, 1992). Recent studies (Lattanzi et al., 2000) have also shown that emerin expression is increased upon differentiation. Ostlund et al. suggested that the absence or severe reduction in emerin or lamin A/C at the nuclear envelope might disrupt interactions with muscle-specific transcription factors or DNA sequences, which are needed in muscle development or regeneration (Ostlund et al., 1999). It also seems likely that there is a cardiac/skeletal muscle protein that interacts specifically with emerin and lamins. One candidate is the A-kinase anchoring proteins (AKAPs) that anchor cyclic-AMP-dependent protein kinase(s) to the nuclear membrane (Eide et al., 1998). They are involved in mitotic chromosome condensation (Hirano et al., 1997; Collas et al., 1999), predominantly in cardiac and skeletal muscle (Kapiloff et al., 1999). Recently, a nuclear matrix protein HA95, which exhibits high homology to the human nuclear A-kinase protein AKAP95, has been shown to interact directly with LAP2β, LBR, emerin and BAF in interphase (Martins et al., 2000). These results support the hypothesis that nuclear complexes, comprising emerin, BAF, lamin and at least one cell-type specific and/or developmentally regulated factor, are involved in gene regulation and that EDMD may specifically arise from the alteration of gene expression in cardiac and skeletal muscle.

An alternative hypothesis is that physical damage to the

nuclear envelope, which has been shown to cause leakage of lamins and chromatin into the cytoplasm (Fidzianska et al., 1998; Ognibene et al., 1999), destabilises the nuclear envelope, which in turn increases fragility leading to the conditions, such as tissue damage and cell death, seen in EDMD patients. Lamin breakdown has been associated with apoptosis (Rao et al., 1996), and recent studies (Cohen et al., 2001; Steen and Collas, 2001) suggest that failure to correctly assemble nuclear lamina triggers apoptosis. As fully differentiated cardiac and skeletal muscle cells are non-dividing, this is of interest because cell death, either by apoptosis or necrosis, may account for the cardiac phenotype. The loss of a few specialised cardiomyocytes in the Purkinje fibres could lead to the conduction abnormalities (Fishbein et al., 1993; Morris, 2000). However, damage to nuclei within the skeletal muscle fibres, which has naturally low levels of lamin B1 (Broers et al., 1997; Ellis, 2001), is more likely to be caused by either the mechanical stresses associated with muscle contraction or a disruption of the skeletal-muscle regeneration process. Trauma to healthy skeletal muscle is characterised by myofibre degeneration followed by the proliferation and differentiation of satellite cells, leading to regeneration of the myofibres (Cullen, 1997). However, in muscular dystrophies, the regeneration process is defective, possibly due to an inability to keep pace with the amount of degeneration occurring. The satellite cells appear to have limited proliferative capacity (Cullen, 1997) and after a few rounds of cell division regeneration fails. Thus, one could predict that skeletal and cardiac muscle types are more sensitive because these cells are unable to cope with reduced levels of protein (emerin, lamin A/C, lamin B1) at the nuclear envelope.

In this study, we have demonstrated that the correct localisation of emerin is important for maintaining nuclear envelope organisation, as the emerin mutants dominantly redistributed a significant amount of lamin A/C. The disruption of this localisation appears to correlate with a lengthening of the cell cycle through a yet to be identified pathway. Thus, changes potentially involving the destablisation of the nuclear envelope caused by mutations in emerin in cardiomyocytes and myofibres may contribute to the pathology of EDMD.

This work was funded by the Medical Research Council (E.A.L.F.) and the Muscular Dystrophy Campaign (J.A.E.). We would like to thank C. J. Hutchison for the lamin A/C antibody, T. P. Hodge for his help with the immunofluorescence imaging and P. Margiotta for help with image illustration.

References

Bione, S., Maestrini, E., Rivella, S., Mancini, M., Regis, S., Romeo, G. and Toniolo, D. (1994). Identification of a novel X-linked gene responsible for Emery-Dreifuss muscular dystrophy. *Nat. Genet.* **8**, 323-327.

Bonne, G., Di Barletta, R. M., Varnous, S., Becane, H.-M., Hammouda, E.-H., Merlini, L., Muntoni, F., Greenberg, C. R., Gary, F., Urtizbera, J.-A. et al. (1999). Mutations in the gene encoding lamin A/C cause autosomal dominant EDMD. *Nat. Genet.* **21**, 285-288.

Broers, J. L., Machiels, B. M., Kuijpers, H. J., Smedts, F., van der Kieboom, R., Raymond, Y. and Ramaekers, F. C. (1997). A- and B-type lamins are differentially expressed in normal human tissue. *Histochem. Cell Biol.* **107**, 505-517.

Broers, J. L. V., Machiels, B. M., van Eys, G. J. J. M., Kuijpers, H. J. H., Manders, E. M. M., van Driel, R. and Ramaekers, F. C. S. (1999). Dynamics of the nuclear lamina as monitoring by GFP-tagged A-type lamins. *J. Cell Sci.* **112**, 3463-3475.

Burke, B. and Gerace, L. (1986). A cell free system to study reassembly of the nuclear envelope at the end of mitosis. *Cell* **44**, 639-652.

Burke, B. (1990). On the cell-free association of lamins A and C with metaphase chromosomes. *Exp. Cell Res.* **186**, 169-176.

Cartegni, L., Di Barletta, R. M., Barresi, R., Squarzomi, S., Sabatelli, P., Maraldi, N., Mora, M., Di Blasi, C., Cornelio, F., Merlini, L. et al. (1997). Heart-specific localization of emerin: new insights into Emery-Dreifuss muscular dystrophy. *Hum. Mol. Genet.* **6**, 2257-2264.

Chaudhary, N. and Courvalin, J.-C. (1993). Stepwise reassembly of the nuclear envelope at the end of mitosis. *J. Cell Biol.* **122**, 295-306.

Chu, A., Rassadi, R. and Stochaj, U. (1998). Velcro in the nuclear envelope: LBR and LAPs. *FEBS Lett.* **441**, 165-169.

Clements, L., Manilal, S., Love, D. R. and Morris, G. E. (2000). Direct interaction between emerin and lamin A. *Biochem. Biophys. Res. Commun.* **267**, 709-714.

Cohen, M., Lee, K. K., Wilson, K. L. and Gruenbaum, Y. (2001). Transcriptional repression, apoptosis, human disease and the functional evolution of the nuclear lamina. *Trends. Biochem. Sci.* **26**, 41-47.

Collard, J.-F., Senecal, J.-L. and Raymond, Y. (1992). Redistribution of nuclear lamin A is an early event associated with differentiation of human promyelocytic leukemia HL-60 cells. *J. Cell Sci.* **101**, 657-670.

Collas, P., Guellec, K. L. and Tasken, K. (1999). The A-kinase-anchoring protein AKAP95 is a multivalent protein with a key role in chromatin condensation in mitosis. *J. Cell Biol.* **147**, 1167-1179.

Collas, P. and Courvalin, J.-C. (2000). Sorting nuclear membrane proteins at mitosis. *Trends Cell Biol.* **10**, 5-8.

Cullen, M. J. (1997). Muscle regeneration. In *Dystrophin-Gene, Protein and Cell Biology* (ed. S.C. Brown and J.A. Lucy), pp. 233-273. Cambridge, Cambridge University Press.

Dabauvalle, M.-C., Loos, K., Merkert, H. and Scheer, U. (1991). Spontaneous assembly of a pore complex-containing membranes ("Annulate lamellae") in *Xenopus* egg extract in the absence of chromatin. *J. Cell Biol.* **112**, 1073-1082.

Dabauvalle, M.-C., Muller, E., Ewald, A., Kress, W., Krohne, G. and Muller, C. R. (1999). Distribution of emerin during the cell cycle. *Eur. J. Cell Biol.* **78**, 749-756.

Dechat, T., Gotzmann, J., Stockinger, A., Harris, C. A., Talle, M. A., Siekierka, J. J. and Foisner, R. (1998). Detergent-salt resistance of LAP2α in interphase nuclei and phosphorylation-dependent association with chromosomes early in nuclear assembly implies function in nuclear structure dynamics. *EMBO J.* **17**, 4887-4902.

Dechat, T., Korbei, B., Vaughan, A., Vlcek, S., Hutchison, C. J. and Foisner, R. (2000a). Lamina-associated polypeptide 2α binds intranuclear A-type lamins. *J. Cell Sci*. **113**, 3473-3484.

Dechat, T., Vlcek, S. and Foisner, R. (2000b). Review: Lamina-associated polypeptide 2 isoforms and related proteins in cell cycle-dependant nuclear structure dynamics. *J. Struct. Biol.* **129**, 335-345.

Di Barletta, R. M., Ricci, E., Galluzz, G., Tonali, P., Mora, M., Morandi, L., Romorini, A., Voit, T., Orstavik, K. H., Merlini, L. et al. (2000). Different mutations in the LMNA gene cause autosomal dominant and autosomal recessive Emery-Dreifuss muscular dystrophy. *Am. J. Hum. Genet.* **66**, 1407-1412.

Drummond, S., Ferrigno, P., Lyon, C., Murphy, J., Goldberg, M., Allen, T., Smythe, C. and Hutchison, C. J. (1999). Temporal differences in the appearance of NEP-B78 and an LBR-like protein during *Xenopus* nuclear envelope reassembly reflect the ordered recruitment of functionally discrete vesicle types. *J. Cell Biol.* **144**, 225-240.

Duband-Goulet, I. and Courvalin, J.-C. (2000). Inner nuclear membrane protein LBR preferentially interacts with DNA secondary structures and nucleosomal linker. *Biochem.* **39**, 6483-6488.

Eide, T., Coghlan, V., Orstavik, S., Holsve, C., Solberg, R., Skalhegg, B. S., Lamb, N. J., Langeberg, L., Fernandez, L., Scott, J. D. et al. (1998). Molecular cloning, chromosomal localization, and cell cycle-dependent subcellular distribution of the A-kinase anchoring protein, AKAP95. *Exp. Cell Res.* **238**, 305-316.

Ellis, D. J., Jenkins, H., Whitfield, W. G. F. and Hutchison, C. J. (1997). GST-lamin fusion proteins act as dominant negative mutants in *Xenopus* egg extract and reveal the function of the lamina in DNA replication. *J. Cell Sci.* **110**, 2507-2518.

Ellis, J., Craxton, M., Yates, J. R. W. and Kendrick-Jones, J. (1998). Aberrant intracellular targeting and cell cycle-dependent phosphorylation of emerin contribute to the Emery-Dreifuss muscular dystrophy phenotype. *J. Cell Sci.* **111**, 781-792.

Ellis, J. A., Yates, J. R. W., Kendrick-Jones, J. and Brown, C. A. (1999).

Changes at P183 of emerin weaken its protein-protein interactions resulting in X-linked EDMD. *Hum. Genet.* **104**, 262-268.

Ellis, J. A. (2001). 81st ENMC International workshop: 4th meeting on Emery-Dreifuss muscular dystrophy, 7th and 8th July 2000, Naarden, The Netherlands. *Neuromuscular Disord.* **11**, 417-420.

Emery, A. E. H. (1989). Emery-Dreifuss syndrome. *J. Med. Genet.* **26**, 637-641.

Emery, A. E. H. (1996). Duchenne and other X-linked muscular dystrophies. In *Principles and Practices of Medical Genetics*, 3rd edn (ed. D. L. Rimon, J. M. Connor and R.E. Pyeritz), pp. 2337-2354. Churchill Livingstone.

Fairley, E. A. L., Kendrick-Jones, J. and Ellis, J. A. (1999). The Emery-Dreifuss muscular dystrophy phenotype arises from aberrant targeting and binding of emerin at the inner nuclear envelope. *J. Cell Sci.* **112**, 2571-2582.

Fidzianska, A., Toniolo, D. and Hausmanowa-Petrusewicz, I. (1998). Ultrastructural abnormality of sarcolemmal nuclei in Emery-Dreifuss muscular dystrophy (EDMD). *J. Neurol. Sci.* **159**, 88-93.

Fishbein, M. C., Siegel, R. J., Thompson, C. E. and Hopkins, L. C. (1993). Sudden death of a carrier of X-linked Emery-Dreifuss muscular dystrophy. *Ann. Int. Med.* **119**, 900-905.

Foisner, R. and Gerace, L. (1993). Intergral membrane proteins of the nuclear envelope interact with lamins and chromosomes, and binding is modulated by mitotic phosphorylation. *Cell* **73**, 1267-1279.

Funakoshi, M., Tsuchiya, Y. and Arahata, K. (1999). Emerin and cardiomyopathy in Emery-Dreifuss muscular dystrophy. *Neuromuscular Disord.* **9**, 108-114.

Furukawa, K. (1999). LAP2 binding protein 1 (L2BP1/BAF) is a candidate mediator of LAP2-chromatin interaction. *J. Cell Sci.* **112**, 2485-2492.

Furukawa, K. and Kondo, T. (1998). Identification of the lamina-associated-polypeptide-2-binding domain of B-type lamin. *Eur. J. Biochem.* **251**, 729-733.

Furukawa, K., Glass, C. and Kondo, T. (1997). Characterization of the chromatin binding activity of lamina-associated polypeptide (LAP) 2. *Biochem. Biophys. Res. Commun.* **238**, 240-246.

Gerace, L. and Blobel, G. (1980). The nuclear envelope lamina is reversibly depolymerized during mitosis. *Cell* **19**, 277-287.

Glass, C. A., Glass, J. R., Taniura, H., Hasel, K. W., Blevitt, J. M. and Gerace, L. (1993). The α-helical rod domain of human lamins A and C contains a chromatin binding site. *EMBO J.* **12**, 4413-4424.

Haraguchi, T., Koujin, T., Hayakawa, T., Kaneda, T., Tsutsumi, C., Imamoto, N., Akazawa, C., Sukegawa, J., Yoneda, Y. and Hiraoka, Y. (2000a). Live fluorescence imaging reveals early recruitment of emerin, LBR, RanBP2, and Nup153 to reforming functional nuclear envelopes. *J. Cell Sci.* **113**, 779-794.

Haraguchi, T., Koujin, T., Segura, M., Wilson, K. L. and Hiraoka, Y. (2000b). Dynamic behavior of emerin and BAF at early stages of nuclear assembly in living HeLa cells. *Mol. Biol. Cell* **11 Suppl.**, 109a.

Hirano, T., Kobayashi, R. and Hirano, M. (1997). Condensins, chromosome condensation protein complexes containing XCAP-C, XCAP-E and a *Xenopus* homolog of the *Drosophila* Barren protein. *Cell* **89**, 511-521.

Hoeltzenbein, M., Karow, T., Zeller, J. A., Warzok, R., Wulff, K., Zshiesche, M., Herrmann, F. H., Große-Heitmeyer, W. and Wehnert, M. S. (1999). Severe clinical expression in X-linked Emery-Dreifuss muscular dystrophy. *Neuromuscular Disord.* **9**, 166-170.

Hoger, T. H., Krohne, G. and Kleinschmidt, J. A. (1991). Interaction of *Xenopus* lamins A and L_{11} with chromatin in vitro mediated by a sequence element in the carboxyterminal domain. *Exp. Cell Res.* **197**, 280-289.

Hugo, P., Kappler, J. W., Godfrey, D. I. and Marrack, P. C. (1992). A cell line that can induce thymocyte positive selection. *Nature* **360**, 679-682.

Hutchison, C. J., Alvarez-Reyes, M. and Vaughan, O. A. (2001). Lamins in disease: why do ubiquitously expressed nuclear envelope proteins give rise to tissue-specific disease phenotypes. *J. Cell Sci.* **114**, 9-14.

Jenkins, H., Holman, T., Lyon, C., Lane, B., Stick, R. and Hutchison, C. (1993). Nuclei that lack a lamina accumulate karyophilic proteins and assemble a nuclear matrix. *J. Cell Sci.* **106**, 275-285.

Kapiloff, M. S., Schillace, R. V., Westphal, A. M. and Scott, J. D. (1999). mAKAP: an A-kinase anchoring protein targeted to the nuclear membrane of differentiated myocytes. *J. Cell Sci.* **112**, 2725-2736.

Klauck, S. M., Wigenbus, P., Yates, J. R. W., Muller, C. R. and Pouska, A. (1995). Identification of novel mutations in three families with Emery-Dreifuss muscular dystrophy. *Hum. Mol. Genet.* **4**, 1853-1857.

Lattanzi, G., Ognibene, A., Sabatelli, P., Capanni, C., Toniolo, D., Columbaro, M., Santi, S., Riccio, M., Merlini, L., Maraldi, N. M. et al. (2000). Emerin expression at the early stages of myogenic differentiation. *Differentiation* **66**, 208-217.

Lin, F., Blake, D. L., Callebaut, I., Skerjanc, I. S., Holmer, L., McBurney, M. W., Paulin-Levasseur, M. and Worman, H. J. (2000). MAN1, an inner nuclear membrane protein that shares the LEM Domain with lamina-associated polypeptide 2 and emerin. *J. Biol. Chem.* **275**, 4840-4847.

Lourim, D. and Lin, J. J.-C. (1989). Expression of nuclear lamin A and muscle-specific proteins in differentiating muscle cells in ovo and in vitro. *J. Cell Biol.* **109**, 495-504.

Lourim, D. and Lin, J. J.-C. (1992). Expression of wild-type and nuclear localization-deficient human lamin A in chick myogenic cells. *J. Cell Sci.* **103**, 863-874.

Lourim, D. and Krohne, G. (1993). Membrane-associated lamins in *Xenopus* egg extracts: identification of two vesicle populations. *J. Cell Biol.* **123**, 501-512.

Lourim, D. and Krohne, G. (1994). Lamin-dependent nuclear envelope reassembly following mitosis: an argument. *Trends. Cell Biol.* **4**, 314-318.

Maison, C., Pyrpasopoulou, A., Theodoropoulos, P. A. and Georgatos, S. D. (1997). The inner nuclear membrane protein LAP1 forms a native complex with B-type lamins and partitions with spindle-associated mitotic vesicles. *EMBO J.* **16**, 4839-4850.

Manilal, S., thi Man, N., Sewry, C. and Morris, G. E. (1996). The Emery-Dreifuss muscular dystrophy protein, emerin, is a nuclear membrane protein. *Hum. Mol. Genet.* **5**, 801-808.

Manilal, S., Sewry, C. A., thi Man, N., Muntoni, F. and Morris, G. E. (1997). Diagnosis of X-linked Emery-Dreifuss muscular dystrophy by protein analysis of leucocytes and skin with monoclonal antibodies. *Neuromuscular Disord.* **7**, 63-66.

Manilal, S., Recan, D., Sewry, C. A., Hoeltzenbein, M., Liense, S., Leturcq, F., Deburgrave, N., Barot, J.-C., thi Man, N., Muntoni, F. et al. (1998a). Mutations in Emery-Dreifuss muscular dystrophy and their effects on emerin protein expression. *Hum. Mol. Genet.* **7**, 855-864.

Manilal, S., thi Man, N. and Morris, G. E. (1998b). Colocalisation of emerin and lamins in interphase nuclei and changes during mitosis. *Biochem. Biophys. Co.* **249**, 643-647.

Martins, S. B., Eide, T., Steen, R. L., Jahnsen, T., Skalhegg, B. S. and Collas, P. (2000). HA95 is a protein of chromatin and nuclear matrix regulating nuclear envelope dynamics. *J. Cell Sci.* **113**, 3703-3713.

Meier, J., Campbell, K. H. S., Ford, C. C., Stick, R. and Hutchison, C. J. (1991). The role of lamin LIII in nuclear assembly and DNA replication, in cell-free extracts of *Xenopus* eggs. *J. Cell Sci.* **98**, 271-279.

Meier, J. and Georgatos, S. D. (1994). Type B lamins remain associated with the integral nuclear envelope protein p58 during mitosis: implications for nuclear reassembly. *EMBO J.* **13**, 1888-1898.

Metcalf, J. A., Gallin, J. I., Nauseef, W. M. and Root, R. T. (1996). *Laboratory Manual of Neutrophil Function*, p. 10. New York, Raven Press.

Mical, T. and Monteiro, M. J. (1998). The role of sequences unique to nuclear intermediate filaments in the targeting and assembly of human lamin B: evidence for lack of interaction of lamin B with its putative receptor. *J. Cell Sci.* **111**, 3471-3485.

Moir, R. D., Spann, T. P., Herrmann, H. and Goldman, R. D. (2000a). Disruption of nuclear lamin organization blocks the elongation phase of DNA replication. *J. Cell Biol.* **149**, 1179-1191.

Moir, R. D., Spann, T. P., Lopez-Soler, R. I. and Yoon, M. (2000b). Review: the dynamics of the nuclear lamins during the cell cycle-relationship between structure and function. *J. Struct. Biol.* **129**, 324-334.

Moir, R. D., Yoon, M., Khuon, S. and Goldman, R. D. (2000c). Nuclear lamins A and B1: different pathways of assembly during nuclear envelope formation in living cells. *J. Cell Biol.* **151**, 1155-1168.

Mora, M., Cartegni, L., Di Blasti, C., Di Barresi, R., Bione, S., Barletta, R., Morandi, L., Merlini, L., Nigro, V., Politano, L. et al. (1997). X-linked Emery-Dreifuss muscular dystrophy can be diagnosed from skin biopsy or blood sample. *Ann. Neurol.* **42**, 249-253.

Morris, G. E. (2000). Nuclear proteins and cell death in inherited neuromuscular disease. *Neuromuscular Disord.* **10**, 217-227.

Nagano, A., Koga, R., Ogawa, M., Kurano, Y., Kawada, J., Okada, R., Hayashi, Y. K., Tsukahara, T. and Arahata, K. (1996). Emerin deficiency at the nuclear membrane in patients with Emery-Dreifuss muscular dystrophy. *Nat. Genet.* **12**, 254-256.

Newport, J. and Spann, T. (1987). Disassembly in the nucleus in mitosis extracts: membrane vesicularization, lamin disassembly, and chromosome condensation are independent processes. *Cell* **48**, 219-230.

Newport, J. W., Wilson, K. L. and Dunphy, W. G. (1990). A lamin-

independent pathway for nuclear envelope assembly. *J. Cell Biol.* **111**, 2247-2259.

Nigg, E. A. (1992). Assembly-disassembly of the nuclear lamina. *Curr. Opin. Cell Biol.* **4**, 105-109.

Nikolakaki, E., Meier, J., Simos, G., Georgatos, S. D. and Giannakouros, T. (1997). Mitosis phosphorylation of the lamin B receptor by a serine/arginine kinase and p34 ^{cdc2}. *Am. Soci. Biochem. Mol. Biol.* **272 (10)**, 6208-6213.

Ognibene, A., Sabatelli, P., Petrini, S., Squaroni, S., Riccio, M., Santi, S., Villanova, M., Palmeri, S., Merlini, L. and Maraldi, N. M. (1999). Nuclear changes in a case of X-linked Emery-Dreifuss muscular dystrophy. *Muscle Nerve* **22**, 864-869.

Ostlund, C., Ellenberg, J., Hallberg, E., Lippincott-Schwartz, J. and Worman, H. J. (1999). Intracellular trafficking of emerin, the Emery Dreifuss muscular dystrophy protein. *J. Cell Sci.* **112**, 1709-1719.

Pyrpasopoulou, A., Meier, J., Maison, C., Simos, G. and Georgatos, S. D. (1996). The lamin B receptor (LBR) provides essential chromatin docking sites at the nuclear envelope. *EMBO J.* **15**, 7108-7119.

Rao, L., Perez, D. and White, E. (1996). Lamin proteolysis facilitates nuclear events during apoptosis. *J. Cell Biol*. **135**, 1441-1455

Sakaki, M., Koike, H., Takahashi, N., Sasagawa, N., Tomioka, S., Araharta, K. and Ishiura, S. (2001). Interaction between emerin and nuclear lamins. *J. Biochem. (Tokyo)* **129**, 321-327.

Shoeman, R. L. and Traub, P. (1990). The in vitro DNA-binding properties of purified nuclear lamin proteins and vimentin. *J. Biol. Chem.* **265**, 9055-9061.

Simos, G., Maison, C. and Georgatos, S. D. (1996). Characterization of p18, a component of the lamin B receptor complex and a new integral membrane protein of the avian erythrocyte nuclear envelope. *J. Biol. Chem.* **271**, 12617-12625.

Spann, T. P., Moir, R. D., Goldman, A. E., Stick, R. and Goldman R.D. (1997). Disruption of nuclear lamin organization alters the distribution of replication factors and inhibits DNA synthesis. *J. Cell Biol.* **136**, 1201-1212.

Spann, T. P., Goldman, A. E., Wang, C., Huang, S. and Goldman, R. D. (2000). Nuclear transcription is blocked by disruption of lamin organization. *Mol. Biol. Cell* **11 Suppl.**, 158a.

Steen, R. L. and Collas, P. (2001). Mistargeting of B-type lamins at the end of mitosis: implications on cell survival and regulation of lamins A/C expression. *J. Cell Biol.* **153**, 621-626.

Sullivan, T., Escalante-Alcalde, D., Bhatt, H., Anver, M., Bhat, N., Nagashima, K., Stewart, C. L. and Burke, B. (1999). Loss of A-type lamin expression compromises nuclear envelope integrity leading to muscular dystrophy. *J. Cell Biol.* **147**, 913-920.

Taniura, H., Glass, C. and Gerace, L. (1995). A chromatin binding site in the tail domain of nuclear lamins that interacts with core histones. *J. Cell Biol.* **131**, 33-44.

Tsuchiya, Y., Hase, A., Ogawa, M., Yorifuji, H. and Arahata, K. (1999). Distinct regions specify the nuclear membrane targeting of emerin, the responsible protein for Emery-Dreifuss muscular dystrophy. *Eur. J. Biochem.* **259**, 859-865.

Ulitzur, N., Harel, A., Feinstein, N. and Gruenbaum, Y. (1992). Lamin activity is essential for nuclear envelope assembly in a *Drosophilia* embryo cell-free extract. *J. Cell Biol.* **119**, 17-25.

Ulitzur, N., Harel, A., Goldberg, M., Feinstein, N. and Gruenbaum, Y. (1997). Nuclear membrane vesicle targeting to chromatin in a *Drosophila* embryo cell-free system. *Mol. Biol. Cell* **8**, 1439-1448.

Vigers, G. P. A. and Lohka, M. J. (1991). A distinct vesicle population targets membranes and pore complexes to the nuclear envelope in *Xenopus* eggs. *J. Cell Biol.* **112**, 545-556.

Wiese, C., Goldberg, M. W., Allen, T. D. and Wilson, K. L. (1997). Nuclear envelope assembly in *Xenopus* extracts visualized by scanning EM reveals a transport-dependent 'envelope smoothing' event. *J. Cell Sci.* **110**, 1489-1502.

Worman, H. J., Yuan, J., Blobell, G. and Georgatos, S. D. (1988). A lamin B receptor in the nuclear envelope. *Proc. Natl. Acad. Sci. USA* **85**, 8531-8534.

Worman, H. J., Evans, C. D. and Blobel, G. (1990). The lamin B receptor of the nuclear envelope inner membrane: a polytopic protein with eight potential transmembrane domains. *J. Cell Biol.* **111**, 1535-1542.

Yates, J. R. W., Bagshaw, J., Aksmanovic, V. M. A., Coomber, E., McMahon, R., Whittaker, J. L., Morrison, P. J., Kendrick-Jones, J. and Ellis, J. A. (1999). Genotype-phenotype analysis in X-linked Emery-Dreifuss muscular dystrophy and identification of a missense mutation associated with a milder phenotype. *Neuromuscular Disord.* **9**, 159-165.

Yates, J. R. W. and Wehnert, M. (1999). The Emery-Dreifuss muscular dystrophy mutation database. *Neuromuscular Disord.* **9**, 199.

Ye, Q. and Worman, H. (1996). Interaction between an integral protein of the nuclear envelope inner membrane and human chromodomain proteins homologous to *Drosophila* HP1. *J. Biol. Chem.* **271**, 14653-14656.

Ye, Q., Callebaut, I., Pezhman, A., Courvalin, J.-C. and Worman, H. J. (1997). Domain-specific interactions of human HP1-type chromodomain proteins and inner nuclear membrane protein LBR. *J. Biol. Chem.* **272**, 1483-1489.